Hindawi Publishing Corporation
Advances in Mathematical Physics
Volume 2012, Article ID 762908, 13 pages
doi:10.1155/2012/762908

Research Article

Relativistic Double Barrier Problem with Three Transmission Resonance Regions

A. D. Alhaidari,[1] H. Bahlouli,[1,2] and A. Jellal[1,3,4]

[1] *Saudi Center for Theoretical Physics, Dhahran, Saudi Arabia*
[2] *Physics Department, King Fahd University of Petroleum & Minerals, Dhahran 31261, Saudi Arabia*
[3] *Physics Department, College of Science, King Faisal University, Al-Ahsaa 31982, Saudi Arabia*
[4] *Theoretical Physics Group, Faculty of Sciences, Chouaib Doukkali University, El Jadida 24000, Morocco*

Correspondence should be addressed to A. Jellal, ahmed.jellal@gmail.com

Received 20 March 2012; Accepted 30 May 2012

Academic Editor: Sanith Wijesinghe

We obtain exact scattering solutions of the Dirac equation in 1 + 1 dimensions for a double square barrier vector potential. The potential bottom between the two barriers is chosen to be higher than $2mc^2$, whereas the top of the barriers is at least $2mc^2$ above the bottom. The relativistic version of the conventional double barrier transmission resonances is obtained for energies within $\pm mc^2$ from the height of the barriers. However, due to our judicious choice of potential configuration we also find two more (subbarrier) transmission resonance regions below the conventional one. Both are located within the two Klein energy zones and characterized by resonances that are broader than the conventional ones. The design of our double barrier so as to enable us to establish these two new subbarrier transmission resonance regions is our main finding.

1. Introduction

The basic equation of relativistic quantum mechanics was formulated more than 80 years ago by Paul Dirac [1–3]. It describes the state of electrons in a way consistent with special relativity, requiring that electrons have spin 1/2 and predicting the existence of an antiparticle partner to the electron (the positron). The physics and mathematics of the Dirac equation is very rich, illuminating, and provides a theoretical framework for different physical phenomena that are not present in the nonrelativistic regime such as the Klein paradox, supercriticality (supercritical transmission of a relativistic particle through a potential barrier) [1–7], and the anomalous quantum Hall effect in graphene [8, 9]. It is well known that the Dirac equation has positive as well as negative energy solutions [1–3]. The positive and negative energy subspaces are completely disconnected. This is a general feature of the solution space

of the Dirac equation, which is sometimes overlooked. Since the equation is linear, then the complete solution must be a linear combination of the two. Incorporating the missing part of the negative energy solution, which is not taken into account in the traditional solution, one of the authors (A. D. Alhaidari) gave a new approach to the resolution of the famous Klein paradox within relativistic quantum mechanics [10]. This approach leads to the correct physical and mathematical interpretations of this phenomenon without resort to quantum field theory.

On the other hand, tunneling phenomena played an important role in nonrelativistic quantum mechanics due to its important application in electronic devices [11, 12]. It was Esaki who discovered a characteristic called negative differential resistance (NDR) whereby, for PN junction diodes, the current voltage characteristics has a sharp peak at a certain voltage associated with resonant tunneling. This constituted the first important confirmation that this phenomenon is due to the quantum mechanical tunneling effect of electrons [13–15]. Tunneling is a purely quantum phenomenon that happens in the classically forbidden region; its experimental observation constituted a very important support to the quantum theory. On the other hand, the study of tunneling of relativistic particles through one-dimensional potentials has been restricted to some simple configurations such as δ-potentials and square barriers, mainly, in the study of the possible relativistic corrections to mesoscopic conduction [16] and the analysis of resonant tunneling through multibarrier systems [17]. Relativistic studies of the quark and Dirac particles in 1D periodic potential were also reported separately in [18, 19].

Very recently, electron transport through electrostatic barriers in single and bilayer graphene has been studied using the Dirac equation, and barrier penetration effects analogous to the Klein paradox were noted [20]. The study of transmission resonances in relativistic wave equations in external potentials has been discussed extensively in the literature [21, 22]. In this case, for given values of the energy and shape of the barrier, the probability of transmission reaches unity even if the potential strength is larger than the energy of the particle, a phenomenon that is not present in the nonrelativistic case. The relation between low momentum resonances and supercritical transmission has been established by Dombey and Calogeracos [7] and Kennedy [23]. Some results on the scattering of Dirac particles by a one-dimensional potential exhibiting resonant behavior have also been reported [22–24].

However, recent studies have shown that inducing a finite bandgap in graphene by epitaxially growing it on a substrate is possible [25] and, therefore, its energy dispersion relation is no longer linear in momentum. This process generated gaps in graphene energy spectrum and resulted in a finite effective mass for its charge carriers and opened up nanoelectronic opportunities for graphene. This 2D massless system can then be mapped into an effectively massive 1D one [26] and, consequently, the problem of Klein tunneling of Dirac fermions across a potential can be put on the test, because the potential barriers can be seen as n-p-n junctions of graphene if they are high enough. Under these circumstances, it is interesting to characterize the system behavior by determining the full expressions of the corresponding reflection and transmission coefficients.

Motivated by the above progress, we study in this work the resonant transmission of a beam of relativistic particles through two separated square barriers with elevated potential bottom in between and investigate transmission resonance in this structure [1–3]. Under special conditions, dictated by our judicious choice of potential bottom elevations and barrier heights, we demonstrate the occurrence of three (subbarrier) regions of transmission resonances. One of them is the relativistic extension of the conventional nonrelativistic double

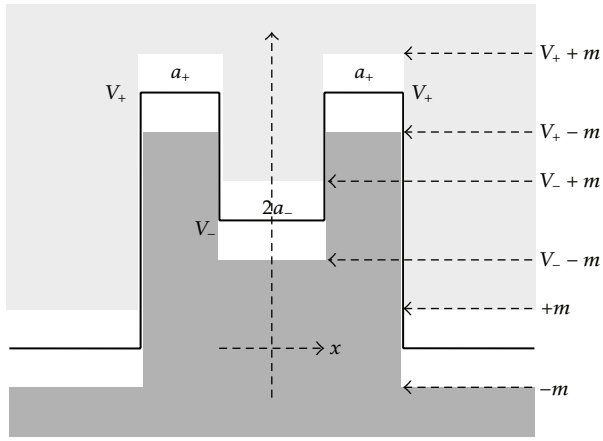

Figure 1: The potential configuration of the relativistic double barrier problem with $V_- > 2m$ and $V_+ > V_- + 2m$. Oscillatory solutions are in the grey regions, whereas exponential solutions are in the white regions. The oscillatory positive/negative energy solutions are located in the light/dark grey areas.

barrier transmission resonances for energies within $\pm mc^2$ from the height of the barriers. The other two are located within the two Klein energy zones where only positive and negative energy oscillatory solutions coexist at the same energy. The latter resonances are broader than the conventional ones.

2. Scattering Solution of the Dirac Equation

The physical configuration associated with the double barrier problem in our study is shown in Figure 1. In the relativistic units $\hbar = c = 1$, the one-dimensional stationary Dirac equation with vector potential coupling can be written as [1–3]

$$\begin{pmatrix} m + V(x) - E & -\dfrac{d}{dx} \\ +\dfrac{d}{dx} & -m + V(x) - E \end{pmatrix} \begin{pmatrix} \psi^+(x) \\ \psi^-(x) \end{pmatrix} = 0, \tag{2.1}$$

where $V(x)$ is the time component of the vector potential whose space component vanishes (i.e., gauged away due to gauge invariance). The potential $V(x)$ is defined by

$$V(x) = \begin{cases} 0 & |x| \geq a_+ + a_-, \\ V_+ & a_- < |x| < a_+ + a_-, \\ V_- & |x| \leq a_-, \end{cases} \tag{2.2}$$

where $V_\pm$ and $a_\pm$ are positive potential parameters (see Figure 1) such that $V_- > 2m$ and $V_+ > V_- + 2m$. We divide configuration space according to the piece-wise constant potential sections into three regions numbered 0 and $\pm$ corresponding to $V = 0$ and $V = V_\pm$, respectively. In

regions 0, where the potential vanishes, the equation becomes the free Dirac equation that relates the two spinor components as follows:

$$\psi^{\mp}(x) = \frac{1}{m \pm E}\frac{d}{dx}\psi^{\pm}(x). \tag{2.3}$$

This relationship is valid for $E \neq \mp m$. Since the problem is linear and because $E = \mp m$ belongs to the $\mp$tive energy spectrum, then (2.3) with the top/bottom sign is valid only for positive/negative energy, respectively. After choosing a sign in (2.3) then the other spinor component obeys the following Schrödinger-like second order differential equation:

$$\left(\frac{d^2}{dx^2} + E^2 - m^2\right)\psi^{\pm}(x) = 0. \tag{2.4}$$

We should emphasize that (2.4) does not give the two components of the spinor that belong to the same energy subspace. One has to choose one sign in (2.4) to obtain only one of the two components then substitute that into (2.3) with the corresponding sign to obtain the other component. Now, within the double barrier (the $V_{\pm}$ regions) the same analysis follows but with the substitution $E \to E - V_{\pm}$ giving

$$\begin{aligned} \psi^{\mp}(x) &= \frac{1}{m \pm (E - V)}\frac{d}{dx}\psi^{\pm}(x), \\ \left[\frac{d^2}{dx^2} + (E - V)^2 - m^2\right]\psi^{\pm}(x) &= 0, \end{aligned} \tag{2.5}$$

where V stands for either of the two potentials $V_{\pm}$. Generally, in any region of constant potential V, positive/negative energy solutions occur for relativistic energies larger/smaller than V. Of these, the oscillatory solutions of the form $e^{\pm i\,kx}$ hold for $|E - V| > m$, where $k^2 = |(E - V)^2 - m^2|$. On the other hand, the exponential solutions of the form $e^{\pm kx}$ hold for $|E - V| < m$.

The scattering solution, which is the subject of this work, pertains to energies $E > m$. It is straightforward to write down the positive and negative energy solutions of (2.3)–(2.5). First, we write the wave vector associated with regions of space in which the potential equals to zero, V_+, and V_-, as

$$k_{\mu}(E) = \sqrt{m^2 - (E - U_{\mu})^2}, \tag{2.6}$$

where $\mu = 0, +, -$ and $U_{\mu} = \{0, V_+, V_-\}$. This results in oscillatory solutions if k_{μ} is pure imaginary which happens when $E > U_{\mu} + m$ or $E < U_{\mu} - m$ (i.e., in the two grey regions of Figure 1). Otherwise, these solutions are exponentials (i.e., in the white areas of the figure). The oscillatory positive/negative energy solutions are located in the light/dark grey areas of Figure 1, respectively. We divide configuration space from left to right into five regions

indexed by $\nu = 1, 2, \ldots, 5$. The general positive energy solution in these regions (both oscillatory and exponentials) can be written as

$$\psi_{\mu,\nu}(x) = \frac{A_\nu}{\sqrt{1+|\alpha_\mu|^2}}\begin{pmatrix}1\\ \alpha_\mu\end{pmatrix}e^{k_\mu x} + \frac{B_\nu}{\sqrt{1+|\alpha_\mu|^2}}\begin{pmatrix}1\\ -\alpha_\mu\end{pmatrix}e^{-k_\mu x}, \tag{2.7a}$$

whereas the negative energy solutions are of the form

$$\psi_{\mu,\nu}(x) = \frac{A_\nu}{\sqrt{1+|\beta_\mu|^2}}\begin{pmatrix}-\beta_\mu\\ 1\end{pmatrix}e^{-k_\mu x} + \frac{B_\nu}{\sqrt{1+|\beta_\mu|^2}}\begin{pmatrix}\beta_\mu\\ 1\end{pmatrix}e^{k_\mu x}. \tag{2.7b}$$

A_ν and B_ν are constants (the complex amplitudes) associated with right and left "traveling" solutions in the νth region, respectively. The energy parameters α_μ and β_μ are defined by

$$\alpha_\mu = \sqrt{\frac{(m - E + U_\mu)}{(m + E - U_\mu)}}, \tag{2.8a}$$

$$\beta_\mu = \sqrt{\frac{(m + E - U_\mu)}{(m - E + U_\mu)}}. \tag{2.8b}$$

Note that $\beta_\mu = \pm 1/\alpha_\mu$ for real/imaginary values, respectively. The complex constant amplitudes $\{A_\nu, B_\nu\}$ will be determined by the boundary conditions. We should note that the oscillatory solutions, $e^{\pm i\,kx}$, in (2.7a) and (2.7b) represent a wave traveling in the $\pm x$ direction for positive energy solutions and in the $\mp x$ direction for negative energy solutions. The solution of the Dirac equation to the right of the double barrier consists of positive energy plane-wave solutions traveling in the $\pm x$ directions. However, the physical boundary conditions of the problem allow only transmitted waves traveling to the right after passing through the double barrier (i.e., $B_5 = 0$). Moreover, and without loss of generality, we can normalize the incident beam to unit amplitude (i.e., $A_1 = 1$).

Matching the spinor wavefunctions at the four boundaries defined by $|x| = a_-$ and $|x| = a_+ + a_-$ gives relations between (A_ν, B_ν) in νth region and those in the neighboring region. We prefer to express these relationships in terms of 2×2 transfer matrices between different regions, $\{M_n\}$, with $\begin{pmatrix}A_n\\ B_n\end{pmatrix} = M_n\begin{pmatrix}A_{n+1}\\ B_{n+1}\end{pmatrix}$. Finally, we obtain the full transfer matrix over the whole double barrier which can be written, in an obvious notation, as follows:

$$\begin{pmatrix}1\\ R\end{pmatrix} = \left(\prod_{n=1}^{4} M_n\right)\begin{pmatrix}T\\ 0\end{pmatrix} = M(E)\begin{pmatrix}T\\ 0\end{pmatrix}, \tag{2.9}$$

where $M(E) = M_1 M_2 M_3 M_4$ and we have set $R = B_1$ and $T = A_5$; R and T being the reflection and transmission amplitudes, respectively. We have assumed an incident wave from left normalized to unit amplitude (i.e., $A_1 = 1$ and $B_5 = 0$). The explicit form of the transfer matrices M_n depends on the specific energy range. There are three such ranges for all $E > m$.

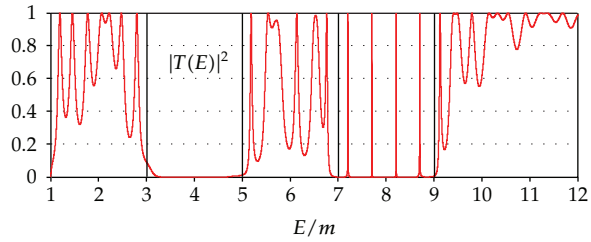

Figure 2: The transmission coefficient as a function of energy associated with the potential configuration of Figure 1 for $V_+ = 8m$, $V_- = 4m$, $a_+ = 3/m$, and $2a_- = 5/m$. Evident are the three subbarrier transmission-resonance regions. The lowest two are within the two Klein energy zones and the highest one with sharp resonances is bounded within the energy range $V_+ \pm m$.

These ranges are (i) $m < E < V_-$, (ii) $V_- < E < V_+$, and (iii) $E > V_+$. Therefore, we end up with the full set of twelve transfer matrices given in the Appendix. Equation (2.9) leads to

$$T(E) = \frac{1}{M_{11}(E)}, \qquad R(E) = \frac{M_{21}(E)}{M_{11}(E)}. \tag{2.10}$$

Time reversal invariance and the relevant conservation laws dictate that the transfer matrix $M(E)$ has a unit determinant along with the following symmetry properties $M_{11}(E) = M_{22}(E)^*$ and $M_{12}(E) = M_{21}(E)^*$, where * stands for complex conjugation. These can easily be checked using the explicit forms given in the Appendix. Thus, symmetry considerations impose strong conditions on the structure of the transfer matrix. Using these properties in (2.10) gives the expected flux conservation $|T|^2 + |R|^2 = 1$. Moreover, from (2.10) we see that full transmission or resonance transmission occurs at energies where the condition $|M_{11}(E)| = 1$ is satisfied (equivalently, $|M_{21}(E)| = 0$).

3. Results and Discussion

The physical content of particle scattering through the double barrier depends on the energy of the incoming particle, which can assume any value larger than m. In order to allow for supercritical transmission through the potential, we need to impose certain conditions on the heights of the potential barriers. Our study concentrates on Klein energy zones where full transmission can take place. The situation of interest to our study concerns two Klein energy zones, which arises when $V_- > 2m$ and $V_+ - V_- > 2m$. As an example, we calculate the transmission coefficient as a function of energy for a given set of potential parameters. The result is shown in Figures 2 and 3. We combine Figures 1 and 2 together in such a way that Figure 2 is turned 90 degrees such that the energy axis of Figures 1 and 2 coincide. In this way, one can clearly see how the different transmission regions correspond to the different potential regions. In addition to the expected above-barrier full transmission for some values of energies larger than $V_+ + m$, one can clearly identify three subbarrier regions where transmission resonances occur. These are

(i) the lower Klein energy zone ($m < E < V_- - m$): a region of seven resonances,

(ii) the higher Klein energy zone ($V_- + m < E < V_+ - m$): a region of four resonances,

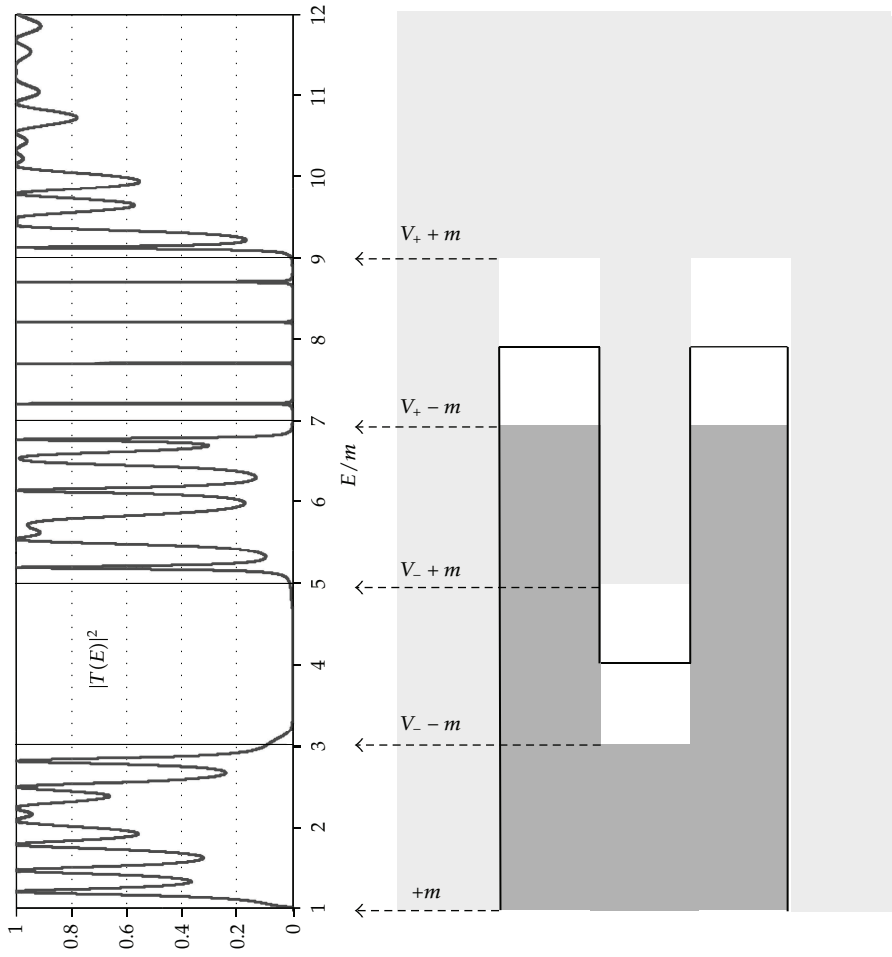

Figure 3: We combine Figures 1 and 2 together in such a way that Figure 2 is turned 90 degrees such that the energy axis of Figures 1 and 2 coincide. In this way, one can clearly see how the different transmission regions correspond to the different potential regions.

(iii) the relativistic version of the conventional nonrelativistic double barrier transmission resonance ($V_+ - m < E < V_+ + m$): a region of four resonances.

It is also clear that resonances in the conventional energy zone are very sharp (or very narrow) whereas those in the two Klein energy zones are broad (or wide). This means that resonance states corresponding to the former decay are much slower and have longer tunneling time than the latter. In Table 1, we list the resonance energies for this potential configuration to an accuracy of 10 decimal places. These results were obtained as solution of the equation $M_{21}(E) = 0$. As further insight into the dynamics of this relativistic model, Figure 4 shows an animation of Figure 2 as the distance between the two barriers, $2a_-$, varies from $2/m$ to $6/m$. The animation shows the following.

(i) The density of resonances in each of the three subbarrier regions increases with a_-, that is, the energy separation between resonances decreases with a_-.

Table 1: Transmission resonance energies (in units of mc^2) for the potential configuration associated with Figure 2 ($V_+ = 8m$, $V_- = 4m$, $a_+ = 3/m$, $a_- = 2.5/m$). These values were obtained as solutions to the equation $M_{21}(E) = 0$.

Level	Lower Klein energy zone	Higher Klein energy zone	Conventional energy zone	Above-barrier energy zone
0	1.1913921248	5.1824247690	7.2022544582	9.1265979020
1	1.4523858967	5.5378483868	7.7033320458	9.4112532302
2	1.7708714661	6.1348174089	8.2103665633	9.4794638424
3	2.0643517404	6.7590893689	8.7007206203	9.7910774141
4	2.2185949080			10.1475989665
5	2.4744005714			10.3256144827
6	2.7966547987			10.5446769142
7				10.9095057090

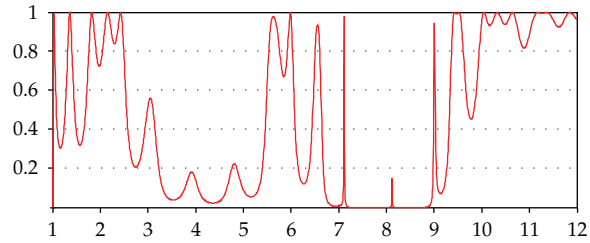

Figure 4: Animation of Figure 2 as the distance between the two barriers, $2a_-$, varies from $2/m$ to $6/m$ (2.4 MB MPG).

(ii) As a_- increases, resonance energies drop down (fall or dive) from the above-barrier region into the conventional resonance region then into the higher Klein energy zone.

(iii) Additionally, as a_- increases, resonance energies are created at the bottom of the spectrum (at $E \approx m$) then move up into the lower Klein energy zone.

Figure 4 gives another animation of Figure 2 as the width of the barriers, a_+, varies from $1/m$ to $3/m$. The animation shows that all resonances get sharper with an increase in a_+ but the number of resonances in the conventional region does not change (i.e., the population density of resonances in this region is independent of a_+). We would like to mention a related recent work by Villalba and Gonzalez-Arraga [27] who considered the resonant tunneling through a double square barrier and double cusp potentials. Our problem differs from that in [27] by the choice of an elevated bottom of the potential well, which gives rise to two Klein energy zones of resonance. This potential design gave rise to a peculiar energy dependence of the transmission with three resonance regions; one is due to the conventional quantum tunneling and two others are due to Klein tunneling. Another animation of Figure 2 is given in Figure 5.

For completeness, it is also interesting to consider the potential barrier with the configuration shown in Figure 6, where $V_+ > 2m$ and $V_- > V_+ + 2m$. The associated transmission coefficient as a function of energy is shown in Figure 7 for the given potential

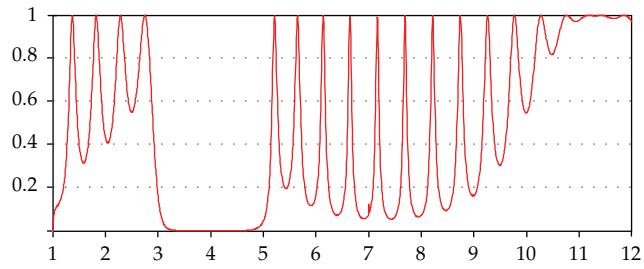

Figure 5: Animation of Figure 2 as the width of the barriers, a_+, varies from $1/m$ to $3/m$ (2.4 MB MPG).

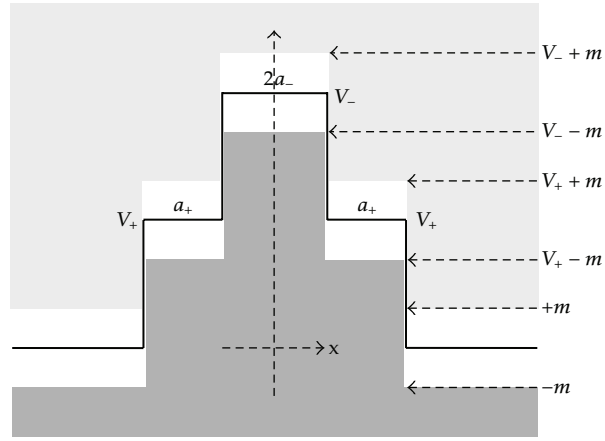

Figure 6: The potential configuration with $V_+ > 2m$ and $V_- > V_+ + 2m$.

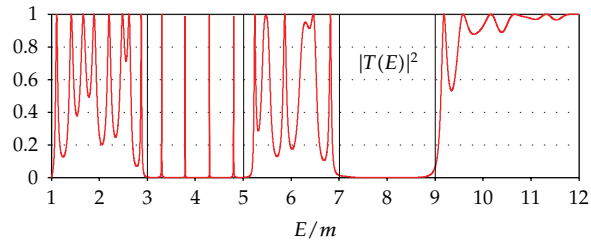

Figure 7: The transmission coefficient associated with the potential configuration of Figure 6 as a function of energy for $V_+ = 4m$, $V_- = 8m$, $a_+ = 3/m$, and $2a_- = 5/m$.

parameters where the values of $V_\pm$ were interchanged. In Figure 8, we combine Figures 6 and 7 together in such a way that Figure 7 is turned 90 degrees such that the energy axis of Figures 6 and 7 coincide. In this way, one can clearly see how the different transmission regions correspond to the different potential regions. It looks as if the energy region $[V_- - m, V_+ + m]$ of Figure 2 was flipped and placed in the energy region $[V_+ - m, V_- + m]$ of Figure 7. Consequently, the sharp resonance region became sandwiched between the two Klein energy zones while the transmission structure of the higher Klein energy zone was reversed.

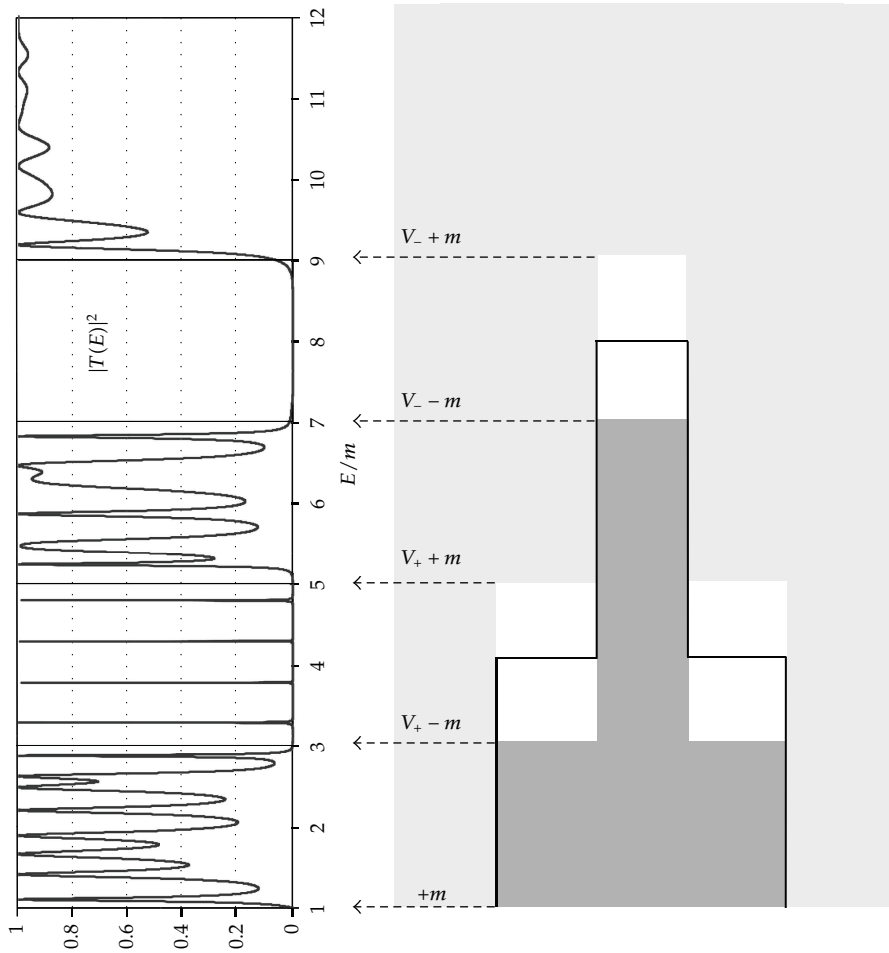

Figure 8: We combine Figures 6 and 7 together in such a way that Figure 7 is turned 90 degrees such that the energy axis of Figures 6 and 7 coincide. In this way, one can clearly see how the different transmission regions correspond to the different potential regions.

Finally, we note that the present work will not remain at this stage but will be pursued further. We plan to use the results obtained so far to deal with different issues related to transport properties in graphene. One of the main characteristics of Dirac fermions in graphene is the accuracy with which we can model their behavior by having extremely small mass (in fact, even massless). This implies that at any finite energy the model should be treated relativistically. This endows fermions in graphene with the ability to tunnel through a single potential barrier with probability one [20, 28–31]. It is then natural to extend that analysis to our two-barrier problem case and investigate the basic features of such a system. However, we would like to mention that graphene is a two-dimensional (2D) system, and 2D carrier tunneling through 1D barriers can be very complicated and direction dependent. Our present results correspond to the transmission of 2D carriers only when the carriers move perpendicular to the potential barriers.

Appendix

Transfer Matrices

If we define $a = a_+ + a_-, \sigma_0 = e^{ak_0}, \sigma_+ = e^{ak_+}$, and $\gamma_\pm = e^{a_-k_\pm}$, then in the first energy interval, $m < E < V_-$, the four transfer matrices at the boundaries $|x| = a_-$ and $|x| = a$ are given by

$$M_1 = \frac{1}{2}\begin{pmatrix} \sigma_0\sigma_+\left(\frac{1}{\alpha_0} - \beta_+\right) & \frac{\sigma_0}{\sigma_+}\left(\frac{1}{\alpha_0} + \beta_+\right) \\ -\frac{\sigma_+}{\sigma_0}\left(\frac{1}{\alpha_0} + \beta_+\right) & \frac{1}{\sigma_0\sigma_+}\left(\beta_+ - \frac{1}{\alpha_0}\right) \end{pmatrix}, \quad M_2 = \frac{1}{2}\begin{pmatrix} \frac{\gamma_-}{\gamma_+}\left(1 + \frac{\beta_-}{\beta_+}\right) & \frac{1}{\gamma_+\gamma_-}\left(1 - \frac{\beta_-}{\beta_+}\right) \\ \gamma_+\gamma_-\left(1 - \frac{\beta_-}{\beta_+}\right) & \frac{\gamma_+}{\gamma_-}\left(1 + \frac{\beta_-}{\beta_+}\right) \end{pmatrix},$$

$$M_3 = \frac{1}{2}\begin{pmatrix} \frac{\gamma_-}{\gamma_+}\left(1 + \frac{\beta_+}{\beta_-}\right) & \gamma_+\gamma_-\left(1 - \frac{\beta_+}{\beta_-}\right) \\ \frac{1}{\gamma_+\gamma_-}\left(1 - \frac{\beta_+}{\beta_-}\right) & \frac{\gamma_+}{\gamma_-}\left(1 + \frac{\beta_+}{\beta_-}\right) \end{pmatrix}, \quad M_4 = \frac{1}{2}\begin{pmatrix} \sigma_0\sigma_+\left(\alpha_0 - \frac{1}{\beta_+}\right) & -\frac{\sigma_+}{\sigma_0}\left(\alpha_0 + \frac{1}{\beta_+}\right) \\ \frac{\sigma_0}{\sigma_+}\left(\alpha_0 + \frac{1}{\beta_+}\right) & \frac{1}{\sigma_0\sigma_+}\left(\frac{1}{\beta_+} - \alpha_0\right) \end{pmatrix}. \tag{A.1}$$

Then, in the second energy range, $V_- < E < V_+$, we have

$$M_1 = \frac{1}{2}\begin{pmatrix} \sigma_0\sigma_+\left(\frac{1}{\alpha_0} - \beta_+\right) & \frac{\sigma_0}{\sigma_+}\left(\frac{1}{\alpha_0} + \beta_+\right) \\ -\frac{\sigma_+}{\sigma_0}\left(\frac{1}{\alpha_0} + \beta_+\right) & \frac{1}{\sigma_0\sigma_+}\left(\beta_+ - \frac{1}{\alpha_0}\right) \end{pmatrix}, \quad M_2 = \frac{1}{2}\begin{pmatrix} \frac{1}{\gamma_+\gamma_-}\left(\alpha_- - \frac{1}{\beta_+}\right) & -\frac{\gamma_-}{\gamma_+}\left(\alpha_- + \frac{1}{\beta_+}\right) \\ \frac{\gamma_+}{\gamma_-}\left(\alpha_- + \frac{1}{\beta_+}\right) & \gamma_+\gamma_-\left(\frac{1}{\beta_+} - \alpha_-\right) \end{pmatrix},$$

$$M_3 = \frac{1}{2}\begin{pmatrix} \frac{1}{\gamma_+\gamma_-}\left(\frac{1}{\alpha_-} - \beta_+\right) & \frac{\gamma_+}{\gamma_-}\left(\frac{1}{\alpha_-} + \beta_+\right) \\ -\frac{\gamma_-}{\gamma_+}\left(\frac{1}{\alpha_-} + \beta_+\right) & \gamma_+\gamma_-\left(\beta_+ - \frac{1}{\alpha_-}\right) \end{pmatrix}, \quad M_4 = \frac{1}{2}\begin{pmatrix} \sigma_0\sigma_+\left(\alpha_0 - \frac{1}{\beta_+}\right) & -\frac{\sigma_+}{\sigma_0}\left(\alpha_0 + \frac{1}{\beta_+}\right) \\ \frac{\sigma_0}{\sigma_+}\left(\alpha_0 + \frac{1}{\beta_+}\right) & \frac{1}{\sigma_0\sigma_+}\left(\frac{1}{\beta_+} - \alpha_0\right) \end{pmatrix}. \tag{A.2}$$

Note that M_1 and M_4 have the same form as in (A.1). Finally, in the energy range, $E > V_+$, we obtain

$$M_1 = \frac{1}{2}\begin{pmatrix} \frac{\sigma_0}{\sigma_+}\left(1 + \frac{\alpha_+}{\alpha_0}\right) & \sigma_0\sigma_+\left(1 - \frac{\alpha_+}{\alpha_0}\right) \\ \frac{1}{\sigma_0\sigma_+}\left(1 - \frac{\alpha_+}{\alpha_0}\right) & \frac{\sigma_+}{\sigma_0}\left(1 + \frac{\alpha_+}{\alpha_0}\right) \end{pmatrix}, \quad M_2 = \frac{1}{2}\begin{pmatrix} \frac{\gamma_+}{\gamma_-}\left(1 + \frac{\alpha_-}{\alpha+}\right) & \gamma_+\gamma_-\left(1 - \frac{\alpha_-}{\alpha+}\right) \\ \frac{1}{\gamma_+\gamma_-}\left(1 - \frac{\alpha_-}{\alpha+}\right) & \frac{\gamma_-}{\gamma_+}\left(1 + \frac{\alpha_-}{\alpha+}\right) \end{pmatrix},$$

$$M_3 = \frac{1}{2}\begin{pmatrix} \frac{\gamma_+}{\gamma_-}\left(1 + \frac{\alpha_+}{\alpha_-}\right) & \frac{1}{\gamma_+\gamma_-}\left(1 - \frac{\alpha_+}{\alpha_-}\right) \\ \gamma_+\gamma_-\left(1 - \frac{\alpha_+}{\alpha_-}\right) & \frac{\gamma_-}{\gamma_+}\left(1 + \frac{\alpha_+}{\alpha_-}\right) \end{pmatrix}, \quad M_4 = \frac{1}{2}\begin{pmatrix} \frac{\sigma_0}{\sigma_+}\left(1 + \frac{\alpha_0}{\alpha_+}\right) & \frac{1}{\sigma_0\sigma_+}\left(1 - \frac{\alpha_0}{\alpha_+}\right) \\ \sigma_0\sigma_+\left(1 - \frac{\alpha_0}{\alpha_+}\right) & \frac{\sigma_+}{\sigma_0}\left(1 + \frac{\alpha_0}{\alpha_+}\right) \end{pmatrix}. \tag{A.3}$$

Acknowledgments

This work is sponsored by the Saudi Center for Theoretical Physics (SCTP). The authors also acknowledge the support provided by King Fahd University of Petroleum & Minerals under Group Projects RG1108-1 and RG1108-2.

References

[1] W. Greiner, *Relativistic Quantum Mechanics: Wave Equations*, Springer, Berlin, Germany, 1994.
[2] J. D. Bjorken and S. D. Drell, *Relativistic Quantum Mechanics*, McGraw-Hill, New York, NY, USA, 1964.
[3] W. Greiner, B. Müller, and J. Rafelski, *Quantum Electrodynamics of Strong Fields*, Springer, Berlin, Germany, 1985.
[4] O. Klein, "Die Reflexion von Elektronen an einem Potentialsprung nach der relativistischen Dynamik von Dirac," *Zeitschrift für Physik*, vol. 53, no. 3-4, pp. 157–165, 1929.
[5] N. Dombey, P. Kennedy, and A. Calogeracos, "Supercriticality and transmission resonances in the dirac equation," *Physical Review Letters*, vol. 85, no. 9, pp. 1787–1790, 2000.
[6] T. R. Robinson, "On Klein tunneling in graphene," *American Journal of Physics*, vol. 80, no. 2, p. 141, 2012.
[7] N. Dombey and A. Calogeracos, "Seventy years of the Klein paradox," *Physics Report*, vol. 315, no. 1–4, pp. 41–58, 1999.
[8] Y. Zheng and T. Ando, "Hall conductivity of a two-dimensional graphite system," *Physical Review B*, vol. 65, Article ID 245420, 2002.
[9] V. P. Gusynin and S. G. Sharapov, "Unconventional integer quantum hall effect in graphene," *Physical Review Letters*, vol. 95, no. 14, Article ID 146801, 4 pages, 2005.
[10] A. D. Alhaidari, "Resolution of the Klein paradox," *Physica Scripta*, vol. 83, no. 2, Article ID 025001, 2011.
[11] M. Razavy, *Quantum Theory of Tunneling*, World Scientific, Singapore, 2003.
[12] D. K. Roy, *Quantum Mechanical Tunneling and Its Applications*, World Scientific, Singapore, 1974.
[13] R. Tsu and L. Ezaki, "Tunneling in a finite superlattice," *Applied Physics Letters*, vol. 22, no. 11, p. 562, 1973.
[14] L. L. Chang, L. Esaki, and R. Tsu, "Resonant tunneling in semiconductor double barriers," *Applied Physics Letters*, vol. 24, no. 12, p. 593, 1974.
[15] T. B. Bahder, C. A. Morrison, and J. D. Bruno, "Resonant level lifetime in GaAs/AlGaAs double-barrier structures," *Applied Physics Letters*, vol. 51, no. 14, p. 1089, 1987.
[16] R. K. Su, G. G. Siu, and X. Chou, "Barrier penetration and Klein paradox," *Journal of Physics A*, vol. 26, no. 4, p. 1001, 1993.
[17] C. L. Roy and A. Khan, "Relativistic impacts on tunnelling through multi-barrier systems," *Journal of Physics C*, vol. 5, no. 41, pp. 7701–7708, 1993.
[18] B. H. J. McKellar and G. J. Stephenson Jr., "Relativistic quarks in one-dimensional periodic structures," *Physical Review C*, vol. 35, no. 6, pp. 2262–2271, 1987.
[19] M. Barbier, F. M. Peeters, P. Vasilopoulos, and J. Milton Pereira Jr., "Dirac and Klein-Gordon particles in one-dimensional periodic potentials," *Physical Review B*, vol. 77, no. 11, Article ID 115446, 9 pages, 2008.
[20] M. I. Katsnelson, K. S. Novoselov, and A. K. Geim, "Chiral tunnelling and the Klein paradox in graphene," *Nature Physics*, vol. 2, no. 9, pp. 620–625, 2006.
[21] P. Kennedy and N. Dombey, "Low momentum scattering in the Dirac equation," *Journal of Physics A*, vol. 35, no. 31, pp. 6645–6657, 2002.
[22] Y. Jiang, S. H. Dong, A. Antillon, and M. Lozada-Cassou, "Low momentum scattering of the Dirac particlewith an asymmetric cusp potential," *The European Physical Journal C*, vol. 45, no. 2, pp. 525–528, 2006.
[23] P. Kennedy, "The Woods-Saxon potential in the Dirac equation," *Journal of Physics A*, vol. 35, no. 3, pp. 689–698, 2002.
[24] V. M. Villalba and W. Greiner, "Frustrated pulse-area quantization in accelerated superradiant atom-cavity systems," *Physical Review A*, vol. 67, no. 6, Article ID 052707, 6 pages, 2003.
[25] S. Y. Zhou, G.-H. Gweon, A. V. Fedorov et al., "Substrate-induced bandgap opening in epitaxial graphene," *Nature Materials*, vol. 6, pp. 770–775, 2007.

[26] A. D. Alhaidari, A. Jellal E. B. Choubabi, and H. Bahlouli, "Dynamical mass generation via space compactificationin graphene," In press, http://arxiv.org/abs/1010.3437.
[27] V. M. Villalba and L. A. Gonzalez-Arraga, "Tunneling and transmission resonances of a Dirac particle by a double barrier," *Physica Scripta*, vol. 81, Article ID 025010, 2010.
[28] C. Bai and X. Zhang, "Klein paradox and resonant tunneling in a graphene superlattice," *Physical Review B*, vol. 76, no. 7, Article ID 075430, 7 pages, 2007.
[29] R. Zhu and Y. Guo, "Shot noise in the graphene-based double-barrier structures," *Applied Physics Letters*, vol. 91, no. 25, Article ID 252113, 3 pages, 2007.
[30] J. Milton Pereira, P. Vasilopoulos, and F. M. Peeters, "Graphene-based resonant-tunneling structures," *Applied Physics Letters*, vol. 90, no. 13, Article ID 132122, 3 pages, 2007.
[31] R. Biswas, S. Mukhopadhyay, and C. Sinha, "Biased driven resonant tunneling through a double barrier graphene based structure," *Physica E*, vol. 42, no. 5, pp. 1781–1786, 2010.